Zhao, C, Zhou, Y, Xing, X, Liu, S, Ren, X and Yang, Q

 Precipitation stability and micro-property of (Nb, Ti)C carbides in MMC coating

Article

For more information please contact researchonline@ljmu.ac.uk

Precipitation stability and micro-property of (Nb, Ti)C carbides in MMC coating

ZHAO Changchun[1], ZHOU Yefei[1, 2]*, XING Xiaolei[1], LIU Sha[1], REN Xuejun[3], YANG Qingxiang[1]*

[1.] State Key Laboratory of Metastable Materials Science & Technology, Yanshan University, Qinhuangdao 066004, P. R. China;

[2.] College of Mechanical Engineering, Yanshan University, Qinhuangdao 066004, P. R. China

[3.] School of Engineering, Liverpool John Moores University, Liverpool L3 3AF, UK

* Corresponding author: Tel. +86-335-838-7471, Fax. +86-335-807-4545

E-mail address: qxyang@ysu.edu.cn, yfzhou@ysu.edu.cn

Abstract: Multiple particles reinforced composite coatings have been noticed by many researchers due to its excellent wear resistance. In this work, (Nb,Ti)C multiple carbide reinforced Fe matrix composite coating was prepared. The microstructure and phase structure of the coatings were analyzed by scanning electron microscope (SEM) equipped with an energy-dispersive spectroscopy (EDS), X-ray diffractometer (XRD) and transmission electron microscopy (TEM). The stability, mechanical parameters (Elastic modulus, Bulk modulus and Shear modulus), hardness, brittleness, bonding structures of (Nb,Ti)C and misfit between carbide and Fe matrix were calculated by first principles method. The experimental results show that, core-shell (Nb,Ti)C can be observed in Ti-1 (0.52 wt.% Ti) coating and compared to Ti-0 (0 wt.% Ti), the morphology of carbides in Ti-1 coating is improved. The calculation results show that, the lattice constants, formation energy of (Nb,Ti)C ($Nb_{0.75}Ti_{0.25}C$, $Nb_{0.5}Ti_{0.5}C$ and $Nb_{0.25}Ti_{0.75}C$) and misfit between carbide and Fe matrix are decreased with the decrease of Ti content in the carbide. Moreover, the hardness and brittleness of (Nb,Ti)C carbides are increased. The Nb-C covalent bonds in (Nb,Ti)C carbides act as a dominant factor for their high hardness.

Keywords: (Nb,Ti)C carbide; Morphology; Stability; Micro-properties; Bonding Structures

1 Introduction

Carbide-reinforced metal matrix composite (MMC) coating has been widely applied in surface modification of Fe based materials for its high hardness, excellent wear resistance and advantage of price [1, 2]. Niobium carbide (NbC) is commonly used as a reinforcement phase in MMCs because of its high melting point, extreme hardness, high wear resistance and almost the same density with Fe matrix [3-5]. Therefore, many researchers are attracted to investigate NbC reinforced Fe matrix coating [6-8]. In order to meet the ever-increasing demands for harsh working conditions, the wear resistance of the coating needs to be further improved. In recent years, researchers have tried to produce coatings containing multiple reinforced particles, which has proven to be an effective way to improve the wear resistance of coatings [9-11]. Cao et al. [12] fabricated high-vanadium based hard composite coating synthesized from premixed powders (V, Cr, Mo, Ti, Nb) on ductile iron (DI) substrate. They found that MC (M = V, Ti, Nb) carbides form together and the micro-hardness in both upper alloyed zone and middle melted zone are obviously enhanced. Li et al. [13] prepared TiN–TiB/Ti composite coating and found that the coating presents outstanding mechanical properties at high temperature. Ravnikar et al. [10] fabricated TiB2–TiC–Al ceramics coating by deposition of a precursor powder mixture on an EN AW 6082-T651 aluminum alloy. The wear resistance of the coating has a great improvement and TiB2 in ceramic components increases the flexural strength of the coating. Li et al. [14] produced in-situ multiple (Ti, Nb)C particles reinforced Fe-based composite coatings with different Ti/Nb atomic ratio and they found that the wear resistance of the coating is improved significantly when Ti/Nb = 1.There is no doubt that multiple

carbides can improve the properties of wear resistant coatings, but their inner improvement mechanism should be concerned.

It is commonly recognized that the main factors impacting on wear resistance of carbides reinforced composites coatings are the hardness, size, morphology and distribution of the carbides [15, 16]. While, another important factor is the lattice misfit between the carbides and matrix. Lu et al. [17] create a class of ultrastrong steel alloys, which has both high strength and good ductility, strengthened by high homogeneity distribution of the Ni(Al,Fe) precipitates. The high strength and good ductility of the alloys are partly caused by low misfit between the precipitates and the martensitic matrix, which decreases associated elastic interaction between precipitates and the matrix nearby. Therefore, the misfit between multiple carbide and matrix should be taken into consideration in the investigation of multiple carbide reinforced coatings. The mechanical properties of multiple carbides should also be investigated. However, it may be difficult to investigate multiple element composition reinforced particles in detail only by experimental method. First-principles calculation based on density functional theory (DFT) has a wide range of applications in the structures and properties of doped systems. Xu et al. [18] researched the mechanical parameters of Ti substitutional additions of β-Ta_5Si_3 by theoretical calculation to guide the compositional design and found that the $(Ta_{0.902}Ti_{0.098})_5Si_3$ could achieve the optimum mechanical properties. Farhadizade et al. [19] investigated the mechanical and electronic properties and the phase stability of Ti_7TMN_8 (TM = V, Cr, Mn, Zr, Nb, Mo, Hf, Ta, W, Re and Os) and indicated that the Ti_7VN_8 and Ti_7MnN_8 has the maximum hardness of 30.7 GPa compared to other doped nitrides. Zhang et al. [20] researched mechanical properties of $Fe_{7-x}Cr_xC$ carbide and found that Fe_4Cr_3C carbide has satisfactory mechanical properties. Jang et al. [21] investigated the stability and lattice parameters of (Ti, M)C where M = Nb, V, Mo, W and indicated that (Ti, Mo)C carbide decreases the misfit strain between the carbide and ferrite matrix. It seems that first-principles calculation is an effective way to investigate mechanical and electronic properties of multiple carbide. (Ti, Nb)C carbide, which can improve the wear resistance of coating, has been reported [14]. In their work, the formation mechanism and distribution characteristics of multiple carbides were investigated. However, the improvement mechanism of the multiple carbide and coating is not clear, which can play an important guiding role in the multiple carbide reinforced composite research. In this work, the morphology, crystal structure and precipitation behavior of (Nb,Ti)C carbide were studied. The formation energy, hardness, brittleness of (Nb,Ti)C and misfit between carbide and Fe matrix were calculated. Subsequently, the ionicity, metallicity and covalence of (Nb,Ti)C carbides were also analyzed to learn the bonding structure of (Nb,Ti)C.

2 Experimental methods and computational details

2.1 Experimental methods

The Fe matrix NbC composites coatings with 0wt.% Ti and 0.52wt.% Ti were prepared by gas metal arc welding (GMAW) hardfacing technology. The flux-cored wire was made of graphite, ferrochromium, ferrovanadium, ferromanganese, ferrosilicon, ferroniobium and ferrotitanium powder core covered by low-carbon steel strip of H08A. Two flux-cored wires were deposited on Q235 low-carbon steel plates. And the details of flux-cored wire manufacturing and hardfacing process were based on our previous work [22]. The compositions of the coatings are listed in Table 1. The phase identification of the coatings was carried out on a Rigaku D/Max-2500/PC X-ray diffraction (XRD) with CuKα operating at 40 kV. The hardfacing specimens were etched with 4 % nitric acid alcohol, and the morphologies were observed by field emission scanning electron microscope (FE-SEM; Hitachi, S-4800). The element analysis of (Nb,Ti)C was carried out by energy dispersive spectrometer (EDS; EMAX). The crystal structure of (Nb,Ti)C carbide was observed by transmission electron microscopy (TEM, JEM-2010).

2.2 Computational details

First-principles calculations based on density functional theory (DFT) with ultrasoft pseudopotentials performed by using Cambridge Sequential Total Energy Package (CASTEP) [23] were employed to evaluate some mechanical properties and bond structures of (Nb,Ti)C carbide. The exchange-correlation energy was evaluated by generalized gradient approximation (GGA) with Perdew-Burke-Ernzerhof (PBE) functional[24]. On the basis of convergence tests, plane–wave cutoff energy was set at 540eV and Brillouin zone sampling was set at 16×16×16 Monkhorst-Pack mesh. For the convergence tolerances, the energy, the maximum force, maximum displacement and maximum stress were set as $5 \times 10_{-6}$ eV/atom, 0.01 eV/Å, $5 \times 10_{-4}$ Å and 0.02GPa, respectively. The mechanical parameters of (Nb,Ti)C were carried out by Voigt-Reuss-Hill (VRH) approximation method [25]. Thermo-Calc software was employed to calculate phase diagrams of the coatings (databases: TCFE7). The calculation elements contents were based on compositions of the coatings.

3.1 Microstructure of (Nb,Ti)C carbide

The X-ray diffraction results of the coatings are shown in Fig.1, and both of them are mainly composed of α-Fe phase and MC type carbide. The microstructures of the coatings are shown in Fig.2. From Fig.2 (a), the microstructures of Ti-0 coating are composed by NbC carbide and α-Fe matrix. From Fig.2 (b), the carbides in Ti-1 coatings exhibit a distinct morphology. Granular core-shell carbides can be observed in Ti-1 coating. The desirable granular shape of carbide can restrict stress concentration around the particles [12, 26]. Therefore, compared with T-0 coating, the morphology of carbide in Ti-1 coating is improved. The Nb and Ti contents of core-shell carbide tested by energy dispersive spectrometer are listed in Table 2. It is found that, the content of Ti element in the core of carbide is larger than that in the shell. Meanwhile, in the core of carbide, the atom percentage of Ti element is large than that of Nb element. The bright field TEM micrograph and selected area electron diffraction (SAED) patterns of core-shell carbide are shown in Fig.3. From the electron diffraction patterns, the core and shell of the carbide show a same crystal orientation with a zone axis [011] and both of them have only one suit of electron diffraction pattern, which indicate that the core shell carbide is (Nb,Ti)C carbide with single crystal structure, rather than a mixture of TiC and NbC carbide.

3.2 Precipitation analysis of (Nb,Ti)C

Diagrams of two coatings have been calculated, which are shown in Fig.4. In Ti-0 coating, carbides begin to precipitate at 1702K, slightly lower than the solidification temperature of α-Fe matrix (1706K). In Ti-0 coating, the carbides precipitate in form of eutectic carbide. In Ti-1 coating, the carbides begin to precipitate at 1788K, which is higher than the solidification temperature of α-Fe matrix (1711K). It indicates that the carbides in Ti-1 coating can precipitate in form of primary granular carbide. To achieve a better understand of the effect of element Ti on carbide formation, the Gibbs free energy of formation of TiC and NbC in Ti-1 coating should be learned. The relationships of standard formation energy of NbC and TiC with temperature are revealed by Formula (1), (2) and (3) [14].

$$\Delta G_{TiC}^{0} = -183172 + 10.09T \quad (298 \leq T \leq 1155) \tag{1}$$

$$\Delta G_{TiC}^{0} = -186731 + 13.20T \quad (1155 \leq T \leq 2000) \tag{2}$$

$$\Delta G_{NbC}^{0} = -136900 + 2.43T \quad (298 \leq T \leq 1800) \tag{3}$$

The relationship of actual Gibbs free energy of formation of TiC and NbC with temperature in molten pool can be expressed by Formula (4), (5)[14, 27]:

$$\Delta G_{TiC} = \Delta G_{TiC}^0 - RT \ln\{[Ti\%][C\%]\} \tag{4}$$

$$\Delta G_{NbC} = \Delta G_{NbC}^0 - RT \ln\{[Nb\%][C\%]\} \tag{5}$$

where $_0\Delta G$ and ΔG are the standard and actual Gibbs free energy of formation of TiC and NbC, respectively. In Ti-1 coating, [$Nb\%$], [$Ti\%$] and [$C\%$] are supposed to be the mass fraction of Nb, Ti and C of the coating. In addition, Ti, Nb and C are supposed to have limited impacts by other elements when they form MC carbide. The result of MC carbides in Ti-1 coating is shown in Fig.5. As can be seen, ΔG_{TiC} is obviously lower than ΔG_{NbC} at the same temperature, which indicates that the formation of TiC is easier than that of NbC in the molten pool at the same temperature. Li[14] considered that TiC forms first, and it can act as nucleation center for (Nb, Ti) C carbides during (Nb, Ti)C carbide growth. So it is reasonable to believe that the addition of element Ti can improve the formation ability of (Nb,Ti)C carbides. The matrix solidification temperature of two coatings are similiar (1706K and 1711K). Therefore, the formation sequence of thr carbide and matrix is changed, and the granular primary carbide can be found in Ti-1 coating.

4 Calculated results

4.1 Mechanical parameters and formation energy of (Nb,Ti)C

For the study of (Nb,Ti)C carbides, it is considered that Nb atoms can be substituted by Ti atoms in NbC carbide, which maybe expressed as $Nb_{0.75}Ti_{0.25}C$, $Nb_{0.5}Ti_{0.5}C$ and $Nb_{0.25}Ti_{0.75}C$. Their calculation crystal structures are shown in Fig.6. All of the carbides are face-centered cube with FM-3M space group, in which, each carbide cell contains eight atoms. Besides, the NbC and TiC carbides were also calculated and the calculated results were compared with other published calculated or experimental results to assess the accuracy of computation method on (Nb,Ti)C in this work [7, 21, 28-34]. The bulk (B) and shear (G) modulus were estimated from elastic constant calculation based on VRH (Voigt-Reuss-Hill) approximation. The elastic modulus (E) and poisson's ratio (v) could be obtained from B and G by the following relationship:

$$E = 9BG / (3B + G) \tag{6}$$

$$v = (3B - 2G) / 2(3B + G) \tag{7}$$

and the formation energy (E_{for}) can be calculated by the Eq. (8)[21]:

$$E_{for}^{(Nb,Ti)C} = \frac{1}{m+n+l}(E_{(Nb,Ti)C}^{total} - mE_{Nb}^{bbc} - nE_{Ti}^{hcp} - lE_{C}^{graphite}) \tag{8}$$

where $E_{(Nb,Ti)C}^{total}$ is the bulk unit energy of (Nb,Ti)C carbide; E_{Nb}^{bbc}, E_{Ti}^{hcp} and $E_{C}^{graphite}$ are the energies of the constituent elements in form of body-centered (bbc) Nb, hexagonal close-packed (hcp) Ti and graphite C, respectively; m, n and l are the numbers of Nb atoms, Ti atoms and C atoms in one (Nb,Ti)C unit, respectively. The calculated lattice constants, elastic modulus, bulk modulus, poisson's ratio and formation energy of (Nb,Ti)C are listed in Table3. The lattice constants of (Nb,Ti)C carbides are decreased with the increase of Ti content. The $Nb_{0.5}Ti_{0.5}C$ carbide presents the lattice constants of tetragonal structure, and the similar results

can be found in calculation of (Ti,Nb)B2 [35]. It can be seen in Table3 that, the introduction of Ti atom into (Nb,Ti)C can decrease the formation energy of carbides, which means the replacement of Nb atom by Ti atom in (Nb,Ti)C is energetically favourable.

4.2 Misfit of (Nb,Ti)C with a-Fe matrix

Considering the lattice misfit (δ) between α-Fe and carbide, the lattice parameter decrease of (Nb,Ti)C is of great significance. The crystallographic orientation of the NaCl type carbide with α-Fe is believed to have a Baker-Nutting relationship[36]:

$$(100)_a \| (100)_{(Nb,Ti)C} , \quad [010]_{aFe} \| [011]_{(Nb,Ti)C} , \text{ and the lattice misfit between them can be}$$

obtained by Eq.(9):

$$\delta = (a_{carbide} - \sqrt{2}a_{aFe}) / a_{carbide} \tag{9}$$

where δ is the lattice misfit between carbide and a-Fe; $_{carbide}a$ is the calculated lattice parameter of carbide. The lattice parameters of NbC, $Nb_{0.25}Ti_{0.75}C$ and α-Fe are 4.46 Å, 4.38 Å and 2.87 Å, respectively. The δ of NbC with α-Fe is 8.7%, and the δ of $Nb_{0.25}Ti_{0.75}C$ with α-Fe decreases to 7.3%, which is beneficial to the elastic interaction of carbides with Fe matrix.

4.3 Elastic constants and theoretical hardness of (Nb,Ti)C

The elastic constants and hardness of (Nb,Ti)C carbide, which is important for carbide reinforced wear resistant coating, should be studied. The calculated elastic constants (C_{ij}) are listed in Table 4 and all the carbides obey the mechanical stability criteria of tetragonal: $C_{11}>0$; $C_{33}>0$; $C_{44}>0$; $C_{66}>0$; $C_{11}-C_{12}>0$; $C_{11}+C_{33}-2C_{13}>0$; $2(C_{11}+C_{12})+C_{33}+4C_{13}>0$, which means the introduction of Ti atom into (Nb,Ti)C is mechanically stable. The elastic constants C_{11} and C_{33} are mainly controlled by the bonds parallel to the a-axis and c-axis respectively. From the results in Table 4, the value of C_{33} is bigger than that of C_{11} in $Nb_{0.5}Ti_{0.5}C$, which indicates the bonds parallel to the c-axis are stronger than that of a- axis. Besides, the value of C_{66} is slightly bigger than that of C_{44}, which means that the shear of [100](001) is more difficult than that of [100](010). The hardness of the (Nb,Ti)C carbides, which obviously affect the wear resistance of carbide reinforced metal composite coatings, should be evaluated. In this work, the hardness value of (Nb,Ti)C is difficult to be obtained by experiment due to the changes of chemical composition and crystal orientations[37] of different carbides. The theoretical hardness of (Nb,Ti)C carbides were calculated by Tian's model (Eq. (10))[38] and Xue's model (Eq. (11))[39]:

$$Hv1 = 0.92K^{1.137}G^{0.708} \tag{10}$$

$$Hv2 = 2(K^2G)^{0.583} - 3 \tag{11}$$

$$K = G / B \tag{12}$$

where $Hv1$ and $Hv2$ are the theoretical hardness; K is the Pugh's modulus ratio; B and G are Bulk modulus and Shear modulus, respectively. The calculated results are shown in Fig.7 (a). The hardness value of NbC, TiC and (Nb,Ti)C calculated by two models present similar tendency. As can be seen obviously, the hardness of the carbides are improved significantly by introducing Ti atom into NbC carbide. The hardness of NbC are 24.25GPa and 24.75GPa, which matched well with other experimental and calculated results (24.1GPa, 24.5GPa) [7]. In

addition, the hardness valve of $Nb_{0.25}Ti_{0.75}C$ reaches almost 29GPa by Xue's model. The brittleness of (Nb,Ti)C carbides can be assessed by the Pugh's modulus ratio 'K', and the carbide equipped with brittle character when 'K' is bigger than 0.571. From Fig.7 (b), the brittleness of (Nb,Ti)C is increased by the introduction of Ti atom.

4.4 Bonding structures of (Nb,Ti)C
As known, the mechanical properties of material are closely related to its bonds structure. To learn the bonding situation of carbides, the total and partial electronic density of states (TDOS, PDOS) were calculated, which is shown in Fig.8. It can be seen clearly that the value of DOS at the Fermi level (E_F) are larger than 0 in all carbides, which indicates the metallic character of all carbides, and the metallicity of these carbides can be achieved by Eq.(13) [40]:

$$f_m = \frac{n_m}{n_e} = \frac{k_B T D_f}{n_e} = \frac{0.026 D_f}{n_e} = \frac{0.026 D_f V_{cell}}{N} \tag{13}$$

where $_fD$ is the DOS value of carbides at fermi level; V_{cell} is the volume of carbides; N is the total number of the valance electrons of the carbides; k_B is the Boltzmann constant; T is the temperature; n_m is the thermal excited electrons and n_e is valence electron density of carbides. The calculated results of metallicity are listed in Table 5. From Table 5, the metallicity of (Nb,Ti)C carbides is bigger than those of NbC and TiC, and decreases in the following sequence: $Nb_{0.75}Ti_{0.25}C > Nb_{0.5}Ti_{0.5}C > Nb_{0.25}Ti_{0.75}C$. Besides, Nb-4d and Ti-3d orbits are overlapped with C-2p orbit, which illustrates the formation of Nb-C and Ti-C covalent bonds formed by the p-d hybridization. To understand the contribution of Nb and Ti atoms to the hardness of (Nb,Ti)C carbides, the information of ionicity and electron transfer of atoms in these carbides should be learned. The plots of charge density differences and charge densities along plane (200), which pass through Nb, Ti and C atoms, are shown in Fig.9 and Fig.10. From Fig.9, the electrons transfer between Nb or Ti atoms and C atoms can be seen clearly, which indicates the formation of Nb-C and Ti-C ionic bonds. The detail of charge transfer can be analyzed by the Mulliken populations of the carbides listed in Table 6. From the atomic populations, a decrease of ionicity of Nb and Ti atoms can be seen from $Nb_{0.75}Ti_{0.25}C$ to $Nb_{0.25}Ti_{0.75}C$, however, ionicity of the carbides is increased because of the atomic charges increase of C atoms. The directional bonding of Nb-C and Ti-C can be observed in Fig.10, which means the formation of Nb-C and Ti-C covalent bonds. It is noteworthy that stronger Nb-C covalent bonds can be found in $Nb_{0.5}Ti_{0.5}C$ and $Nb_{0.25}Ti_{0.75}C$ carbides, and these bonds in $Nb_{0.5}Ti_{0.5}C$ carbide are parallel to the c-axis. From the calculated bond populations listed in Table 6, the strengthes of Nb-C and Ti-C covalent bonds in (Nb,Ti)C are increased with the increase of Ti content. (Nb,Ti)C carbides have complex chemical bonding mixing together metallic, covalent, and ionic characters.

5 Discussion
The hardness of (Nb,Ti)C carbides can be improved significantly by introducing Ti atom into NbC carbide. To learn this tendency, bonding analysis is need. (Nb,Ti)C carbides have mixed bonding structures of metallic, covalent, and ionic characters. The metallicity of (Nb,Ti)C carbides is decreased. The ionicity of the carbides is increased. The strengthes of Nb-C and Ti-C covalent bonds in (Nb,Ti)C, which play an important role on the bulk modulus (B) and shear modulus (G) of carbides, are increased with the increase of Ti content. According to Tian's points [38] of microscopic hardness model, ioncity and metallity are adverse for hardness.

However, strong directional covalent bonds could be a considerable factor of supperhard material. Obviously, Nb-C covalent bonds in (Nb,Ti)C carbides act as a dominant factor for their high hardness.

6 Conclusions

(1) The precipitate temperature of the carbide in Ti-1coating is 1788K, which is higher than that in Ti-0 coating at 1706K. The increase of the precipitate temperature changes the formation sequence of the carbide and α-Fe matrix in Ti-1 coating, as a result, the primary carbide can be observed.

(2) The replacement of Nb atom by Ti atom in (Nb,Ti)C decreases the formation energy and the misfit between (Nb,Ti)C and Fe matrix.

(3) The hardness and brittleness are increased by introducing Ti atom into NbC carbide, and the calculated hardness value of $Nb_{0.25}Ti_{0.75}C$ carbide is almost up to 29GPa. Although it has not been compared with experimental hardness values, similar results can be get from two models and the bonding structure analysis results are also supporting the hardness tendency, which may ensure the reliability of calculated hardness results.

(4) The metallicity of carbides is decreased and ionicity of carbides is increased from $Nb_{0.75}Ti_{0.25}C$ to $Nb_{0.25}Ti_{0.75}C$. Nb-C covalent bonds in (Nb,Ti)C carbides act as a dominant factor for their high hardness.

Reference

[1] X.H. Wang, Z.D. Zou, S.Y. Qu, S.L. Song, Microstructure and wear properties of Fe-based hardfacing coating reinforced by TiC particles, Journal of Materials Processing Technology, 168 (2005) 89-94.[2] R. Colaço, R. Vilar, Laser rapid-alloy prototyping for the development of wear resistant Fe–Cr–C/NbC composite materials, Journal of Laser Applications, 15 (2003) 267-272.

[3] Q. Li, Y. Lei, H. Fu, Laser cladding in-situ NbC particle reinforced Fe-based composite coatings
with rare earth oxide addition, Surface and Coatings Technology, 2014) 102-107.

[4] F.-Y. Hung, Z.-Y. Yan, L.-H. Chen, T.-S. Lui, Microstructural characteristics of PTA-overlayed NbC
on pure Ti, Surface and Coatings Technology, 200 (2006) 6881-6887.

[5] Y.-B. Cao, S.-X. Zhi, Q. Gao, X.-T. Tian, T. Geng, X. Guan, C. Qin, Formation behavior of in-situ NbC in Fe-based laser cladding coatings, Materials Characterization, 119 (2016) 159-165.

[6] N. Zhao, Y. Xu, Y. Fu, Mechanical properties of one-step in situ synthesized NbC-Fe composite coating, Surface and Coatings Technology, 309 (2017) 1105-1110.

[7] L. Wu, Y. Wang, Z. Yan, J. Zhang, F. Xiao, B. Liao, The phase stability and mechanical properties of Nb–C system: Using first-principles calculations and nano-indentation, Journal of Alloys and Compounds, 561 (2013) 220-227.

[8] L. Zhong, Y. Xu, F. Ye, In situ NbC particulate-reinforced iron matrix composite: microstructure and abrasive wear characteristics, Tribology Letters, 47 (2012) 253-259.

[9] A.K. Srivastava, K. Das, Microstructure and abrasive wear study of (Ti,W)C-reinforced

high-manganese austenitic steel matrix composite, Materials Letters, 62 (2008) 3947-3950.

[10] D. Ravnikar, N.B. Dahotre, J. Grum, Laser coating of aluminum alloy EN AW 6082-T651 with TiB2 and TiC: Microstructure and mechanical properties, Applied Surface Science, 282 (2013) 914-922.

[11] J. Jung, S. Kang, Sintered (Ti,W)C carbides, Scripta Materialia, 56 (2007) 561-564.

[12] H. Cao, X. Dong, S. Chen, M. Dutka, Y. Pei, Microstructure evolutions of graded high-vanadium tool steel composite coating in-situ fabricated via atmospheric plasma beam alloying, Journal of Alloys and Compounds, 720 (2017) 169-181.

[13] M. Li, J. Huang, Y.Y. Zhu, Z.G. Li, Effect of heat input on the microstructure of in-situ synthesized TiN–TiB/Ti based composite coating by laser cladding, Surface and Coatings Technology, 206 (2012) 4021-4026.

[14] Q. Li, Y. Lei, H. Fu, Growth mechanism, distribution characteristics and reinforcing behavior of (Ti, Nb)C particle in laser cladded Fe-based composite coating, Applied Surface Science, 316 (2014) 610-616.

[15] L. Zhong, F. Ye, Y. Xu, J. Li, Microstructure and abrasive wear characteristics of in situ vanadium carbide particulate-reinforced iron matrix composites, Materials & Design (1980-2015), 54 (2014) 564-569.

[16] S. Wei, Z. Jinhua, X. Liujie, L. Rui, Effects of carbon on microstructures and properties of high vanadium high-speed steel, Materials & Design, 27 (2006) 58-63.

[17] S. Jiang, H. Wang, Y. Wu, X. Liu, H. Chen, M. Yao, B. Gault, D. Ponge, D. Raabe, A. Hirata, M. Chen, Y. Wang, Z. Lu, Ultrastrong steel via minimal lattice misfit and high-density nanoprecipitation, Nature, 544 (2017) 460-464.

[18] J. Xu, J. Cheng, S. Jiang, P. Munroe, Z.-H. Xie, The influence of Ti additions on the mechanical and electrochemical behavior of β-Ta5Si3 nanocrystalline coating, Applied Surface Science, 419 (2017) 901-915.

[19] A.R. Farhadizadeh, A.A. Amadeh, H. Ghomi, The effect of metal transition dopant on electronic and mechanical properties of titanium nitride: First principle method, Computational Materials Science, 141 (2018) 82-90.

[20] P.F. Zhang, Y.F. Zhou, J. Yang, D. Li, X.J. Ren, Y.L. Yang, Q.X. Yang, Optimization on mechanical properties of Fe7−xCrxC3 carbides by first-principles investigation, Journal of Alloys and Compounds, 560 (2013) 49-53.

[21] J.H. Jang, C.-H. Lee, Y.-U. Heo, D.-W. Suh, Stability of (Ti,M)C (M=Nb, V, Mo and W) carbide in steels using first-principles calculations, Acta Materialia, 60 (2012) 208-217.

[22] X. Yun, Y.F. Zhou, B. Zhao, X.L. Xing, J. Yang, Y.L. Yang, Q.X. Yang, Influence of Nano-Y2O3 on
Wear Resistance of Hypereutectic Fe–Cr–C Hardfacing Coating, Tribology Letters, 58 (2015).

[23] D. Vanderbilt, Soft self-consistent pseudopotentials in a generalized eigenvalue formalism, Physical Review B, 41 (1990) 7892-7895.

[24] J.P. Perdew, E.R. McMullen, A. Zunger, Density-functional theory of the correlation energy in atoms and ions: A simple analytic model and a challenge, Physical Review A, 23 (1981) 2785-2789.

[25] W. Boas, Physical properties of crystals, their representation by tensors and matrices : J.F Nye : Clarendon Press, Oxford, 1957. 322pp., 50s.

[26] J.W. Park, C.L. Huo, S. Lee, Composition, microstructure, hardness, and wear properties of high-speed steel rolls, Metallurgical & Materials Transactions A, 30 (1999) 399-409.

[27] Y. Yan, B. Wei, FU. Zhengyi, H. Lin, R. Yuan, In situ TiC particulates reinforced ferrous matrix composite and its microstructure forming mechnism, Acta Metallrugica Sinica, 35 (1999) 1117-1120.

[28] A. Teresiak, H. Kubsch, X-ray investigations of high energy ball milled transition metal carbides, Nanostructured Materials, 6 (1995) 671–674.

[29] A.M. Nartowski, I.P. Parkin, M. Mackenzie, A.J. Craven, Solid state metathesis: synthesis of metal carbides from metal oxides, Journal of Materials Chemistry, 11 (2001) 3116-3119.

[30] Y. Yang, H. Lu, C. Yu, J.M. Chen, First-principles calculations of mechanical properties of TiC and TiN, Journal of Alloys and Compounds, 485 (2009) 542-547.

[31] K. Chen, L. Zhao, Elastic properties, thermal expansion coefficients and electronic structures of Ti0.75X0.25C carbides, Journal of Physics and Chemistry of Solids, 68 (2007) 1805-1811.

[32] X. Fan, B. Chen, M. Zhang, D. Li, Z. Liu, C. Xiao, First-principles calculations on bonding characteristic and electronic property of TiC (111)/TiN (111) interface, Materials & Design, 112 (2016) 282-289.

[33] E.I. Isaev, S.I. Simak, I.A. Abrikosov, R. Ahuja, Y.K. Vekilov, M.I. Katsnelson, A.I. Lichtenstein, B. Johansson, Phonon related properties of transition metals, their carbides, and nitrides: A first-principles study, Journal of Applied Physics, 101 (2007) 123519.

[34] H.W. Hugosson, O. Eriksson, U. Jansson, B. Johansson, Phase stabilities and homogeneity ranges in4d-transition-metal carbides: A theoretical study, Physical Review B, 63 (2001) 134108.

[35] N.R. Mediukh, P.E.A. Turchi, V.I. Ivashchenko, V.I. Shevchenko, First-principles calculations for the mechanical properties of Ti-Nb-B2 solid solutions, Computational Materials Science, 129 (2017) 82-88.

[36] M. Charleux, W.J. Poole, M. Militzer, A. Deschamps, Precipitation behavior and its effect on strengthening of an HSLA-Nb/Ti steel, Metallurgical & Materials Transactions A, 32 (2001) 1635-1647.

[37] Y. Kumashiro, A. Itoh, T. Kinoshita, M. Sobajima, The micro-Vickers hardness of TiC single crystals up to 1500° C, Journal of Materials Science, 12 (1977) 595-601.

[38] Y. Tian, B. Xu, Z. Zhao, Microscopic theory of hardness and design of novel superhard crystals, International Journal of Refractory Metals and Hard Materials, 33 (2012) 93-106.

[39] X.-Q. Chen, H. Niu, D. Li, Y. Li, Modeling hardness of polycrystalline materials and bulk metallic glasses, Intermetallics, 19 (2011) 1275-1281.

[40] Y. Li, Y. Gao, B. Xiao, T. Min, Y. Yang, S. Ma, D. Yi, The electronic, mechanical properties and theoretical hardness of chromium carbides by first-principles calculations, Journal of Alloys and Compounds, 509 (2011) 5242-5249.

Table 1 Compositions of coatings (wt.%)

No.	C	Nb	Cr	Mn	Si	V	Ti	Fe
Ti-0	0.38	4.52	5.40	1.15	1.43	0.57	-	Bal.
Ti-1	0.4	4.49	5.33	1.21	1.50	0.55	0.52	Bal.

Table 2 EDS analysis results of core-shell carbide

Chemical element	Core		Shell	
	Weight percentage	Atom percentage	Weight percentage	Atom percentage
Ti	32.44	43.22	3.09	4.61
Nb	46.60	32.01	58.24	44.72
Fe	16.48	18.83	33.02	42.18
Cr	2.54	3.35	3.70	5.07
Mn	1.94	2.59	2.58	3.42

Table 3 Calculated results of lattice constants, elastic modulus, bulk modulus, shear modulus, passion ratio and formation energy.

Phase	Lattice constants	Elastic modulus	Bulk modulus	Shear modulus	Passion ratio	Formation energy
	a(Å)	E(GPa)	B(GPa)	G(GPa)	v	E_{for} (eV/atom)
NbC	4.46	509	316	206	0.23	-0.63
	4.46[28],4.47[29]	488[7]	318[21]	198[7]	0.22[7]	-0.56[7],-0.71[28]
$Nb_{0.75}Ti_{0.25}C$	4.43	497	297	204	0.22	-0.67
$Nb_{0.5}Ti_{0.5}C$	4.42(a,b)	483	278	204	0.21	-0.72
	4.38(c)					
$Nb_{0.25}Ti_{0.75}C$	4.38	472	258	197	0.195	-0.78
TiC	4.35	416	237	172	0.20	-0.82
	4.33[30]	429[31]	237[32],240[33]	177[31]	0.19[30]	-0.85[21],-0.95[34]

Table 4 Calculated elastic constants C_{ij} of (Nb,Ti)C

Phase	C_{11}	C_{12}	C_{13}	C_{33}	C_{44}	C_{66}
NbC	675.18	137.46	137.46	675.18	173.57	173.57
$Nb_{0.75}Ti_{0.25}C$	639.35	126.02	126.02	639.35	174.64	174.64
$Nb_{0.5}Ti_{0.5}C$	585.67	117.96	116.32	629.01	182.21	185.53
$Nb_{0.25}Ti_{0.75}C$	548.94	113.84	113.84	548.94	185.13	185.13
TiC	474.28	115.62	115.62	474.28	167.40	167.40

Table 5 Calculated cell volume, Dos at Fermi level, the total number of valance electrons, the metallicity of (Nb,Ti)C carbides.

Phase	D_f(states/eV)	V_{cell}(Å^3)	N	f_m
NbC	1.87	88.75	68	0.063
Nb$_{0.75}$Ti$_{0.25}$C	3.89	87.37	67	0.132
Nb$_{0.5}$Ti$_{0.5}$C	3.83	85.82	66	0.129
Nb$_{0.25}$Ti$_{0.75}$C	2.18	84.04	65	0.081
TiC	1.75	82.49	64	0.065

Table 6 Calculated Mulliken overlap population (MOP): Atomic charges (e) and Bond populations.

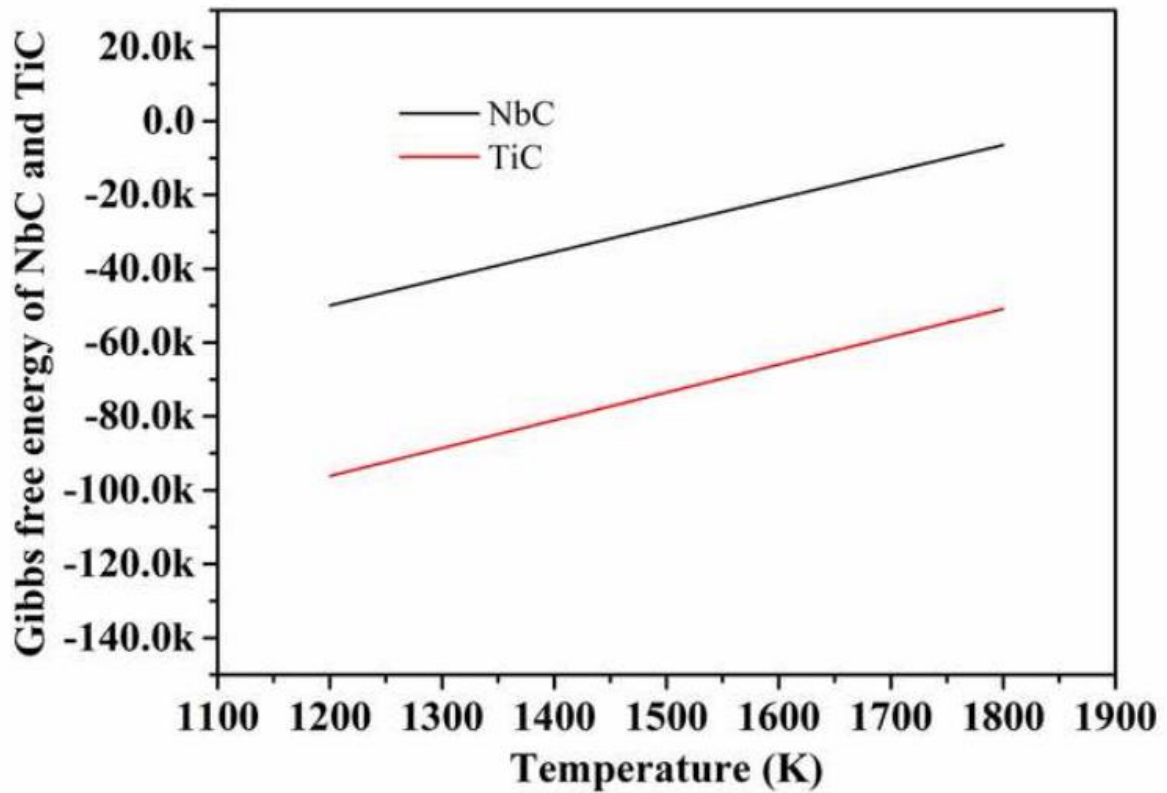|		NbC	Nb$_{0.75}$Ti$_{0.25}$C	Nb$_{0.5}$Ti$_{0.5}$C	Nb$_{0.25}$Ti$_{0.75}$C	TiC
Atomic populations	C	-0.68	-0.69	-0.70	-0.70	-0.71
	Nb	0.68	0.63	0.57	0.49	
	Ti		0.88	0.82	0.77	0.71
Bond populations	Nb-C	0.74	0.90	1.10	1.05	
			0.71	0.84		
	Ti-C		0.59	0.58	0.66	0.82
				0.71	0.89	
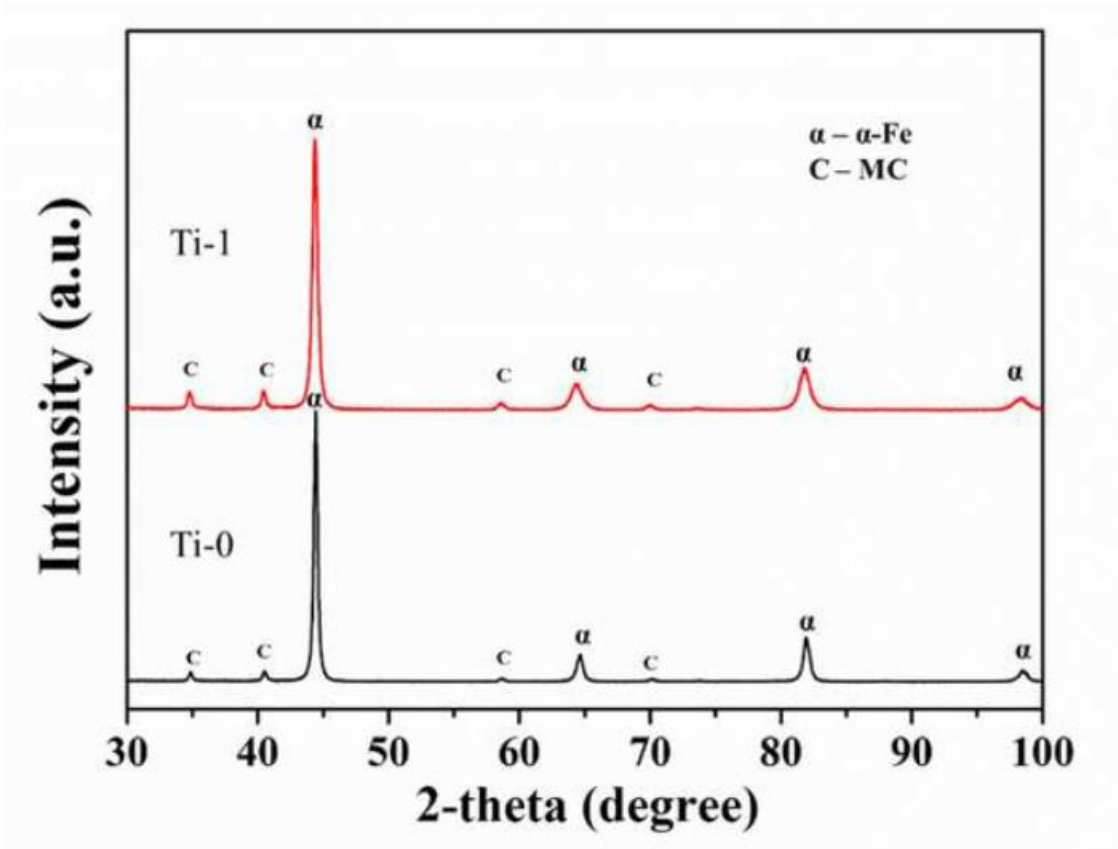
Fig.1. XRD result of coatings.
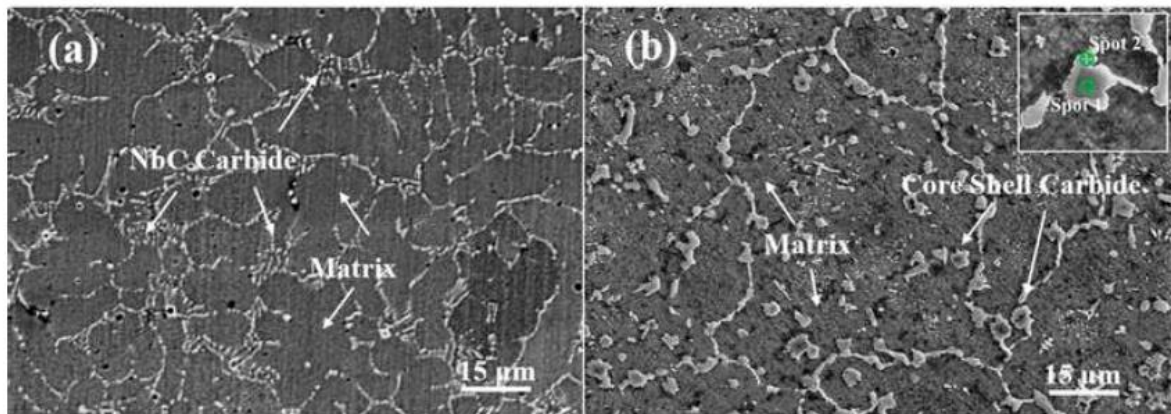
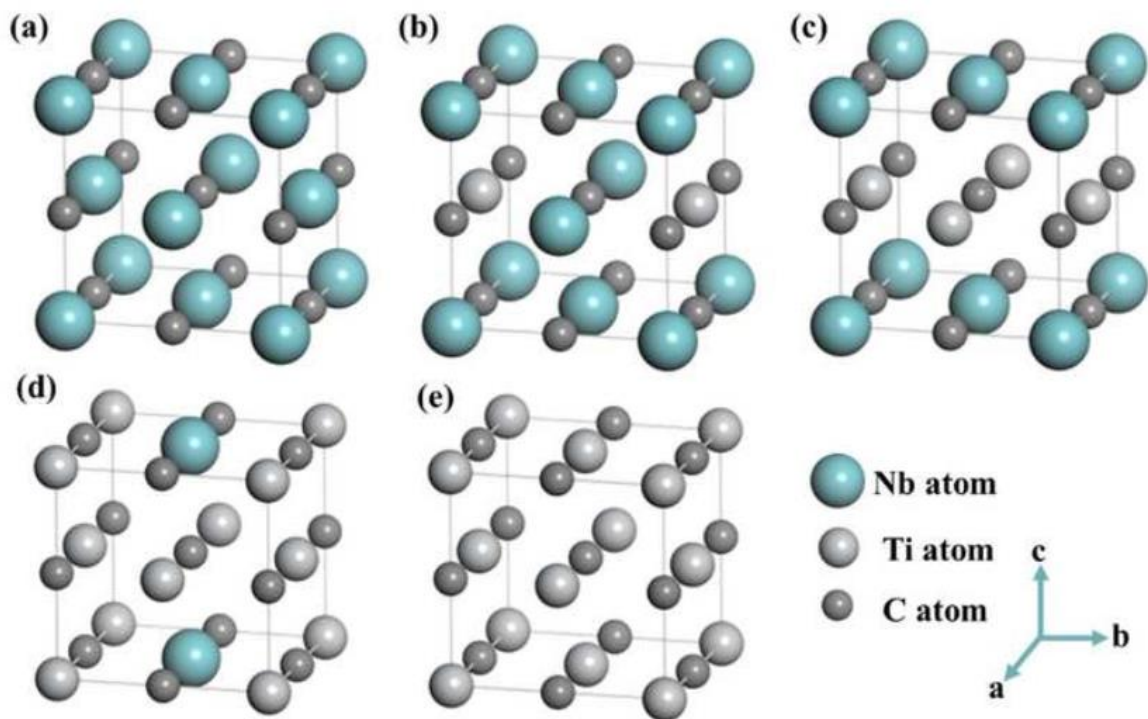**Fig.2.** Morphologies of the coatings. (a) Ti-0 (b) Ti-1
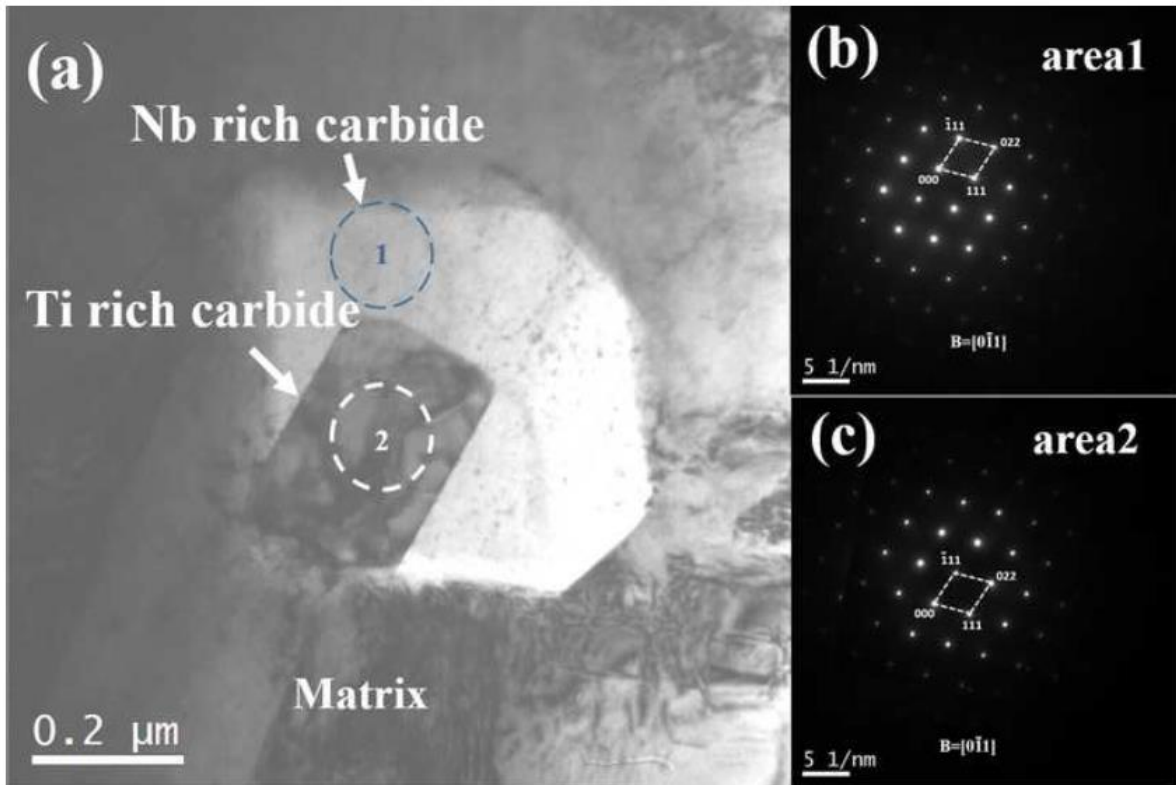
Fig.3. TEM image of (Nb,Ti)C and SEAD pattern of area1 and area2. (a) TEM image of (Nb,Ti)C (b) area1 (c) area2
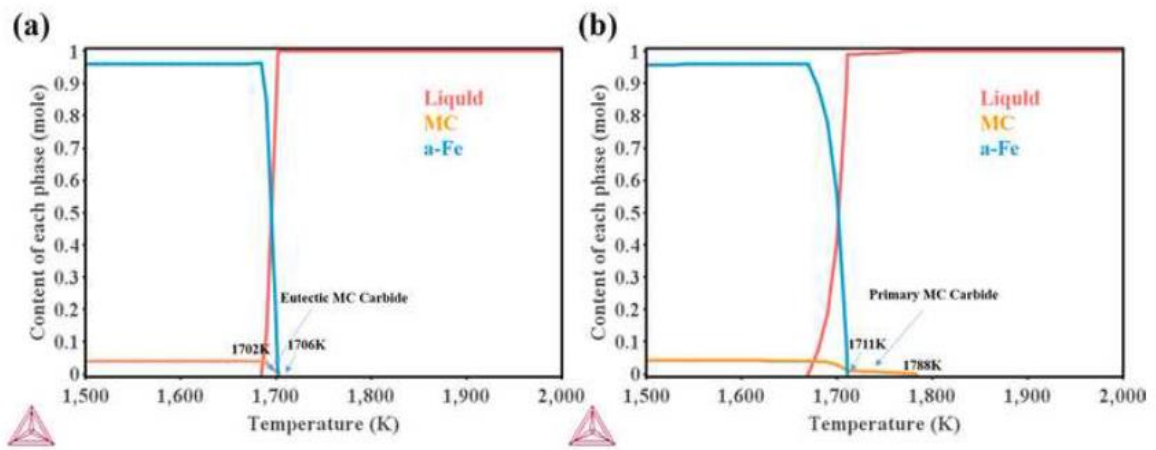
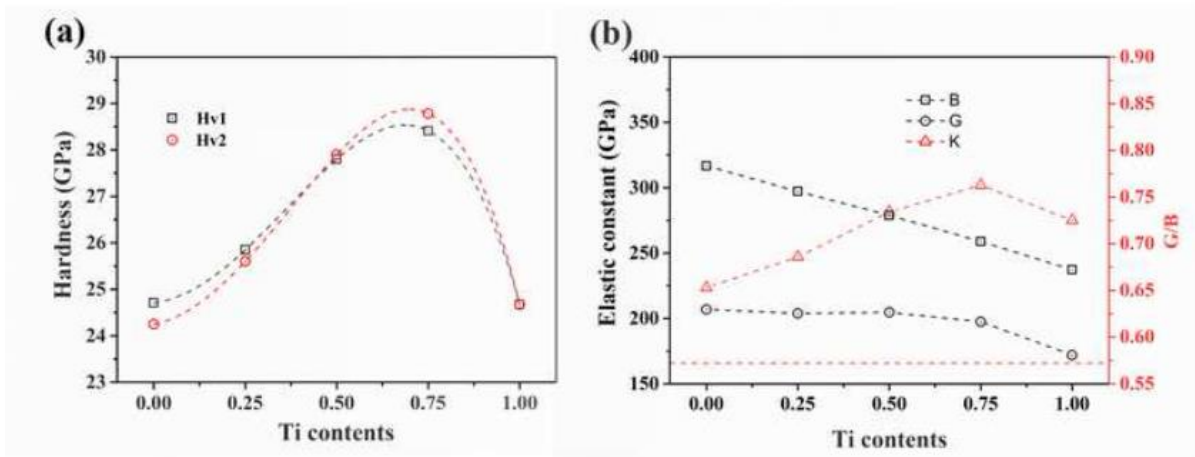**Fig.4.** Diagrams of two coatings. (a) Ti-0 (b) Ti-1

Fig.5. Formation of Gibbs free energy of TiC and NbC in Ti-1 coating
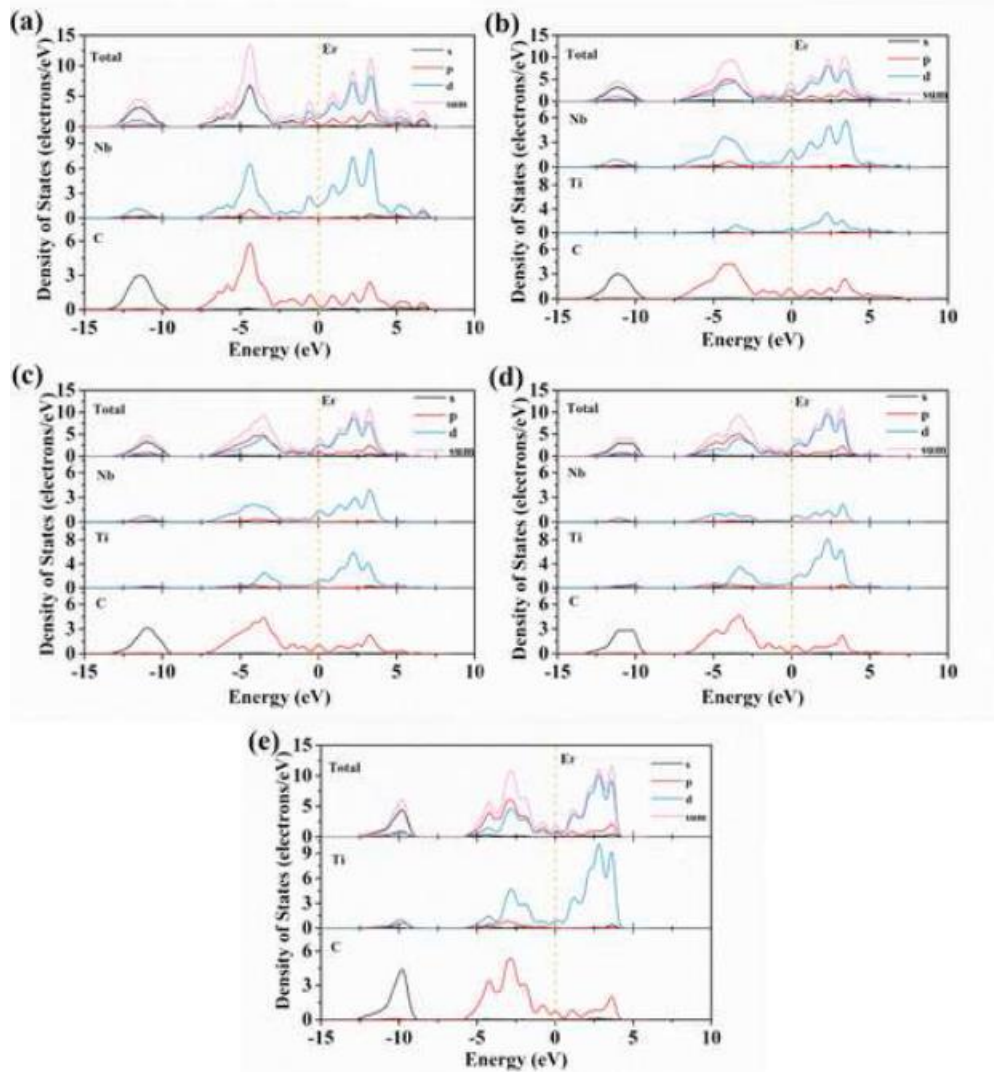

Fig.6. Calculation models of (Nb,Ti)C. (a) NbC (b) $Nb_{0.75}Ti_{0.25}C$ (c) $Nb_{0.5}Ti_{0.5}C$ (d) $Nb_{0.25}Ti_{0.75}C$ (e) TiC
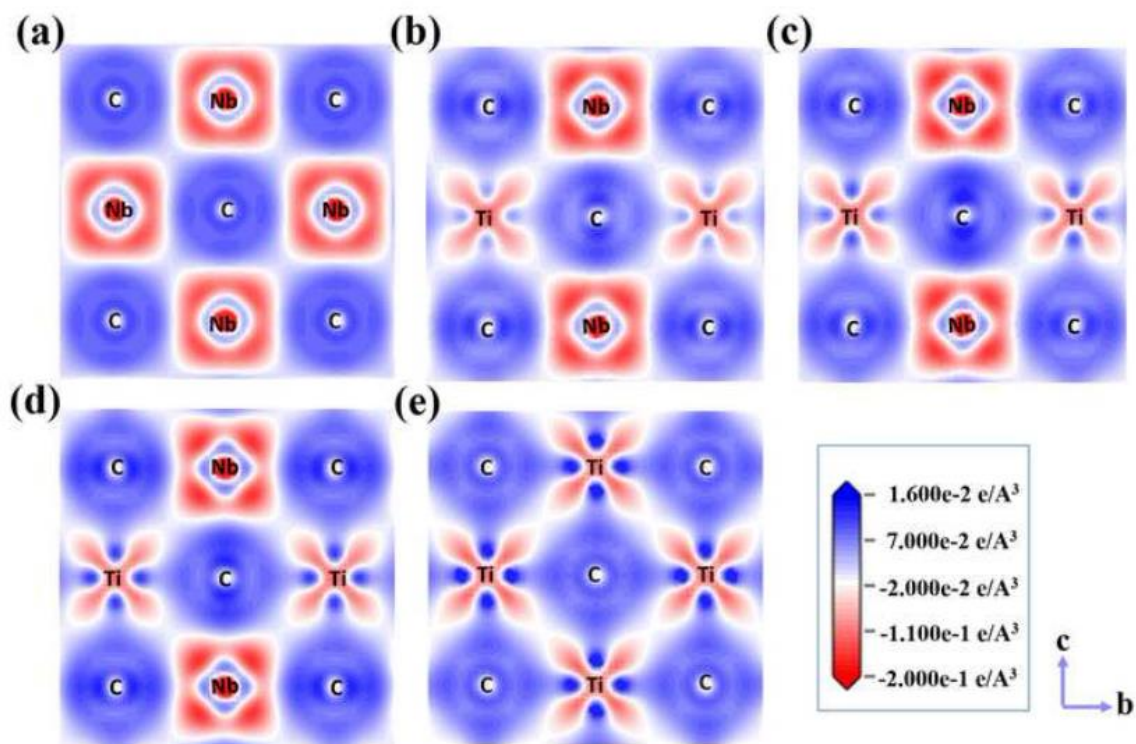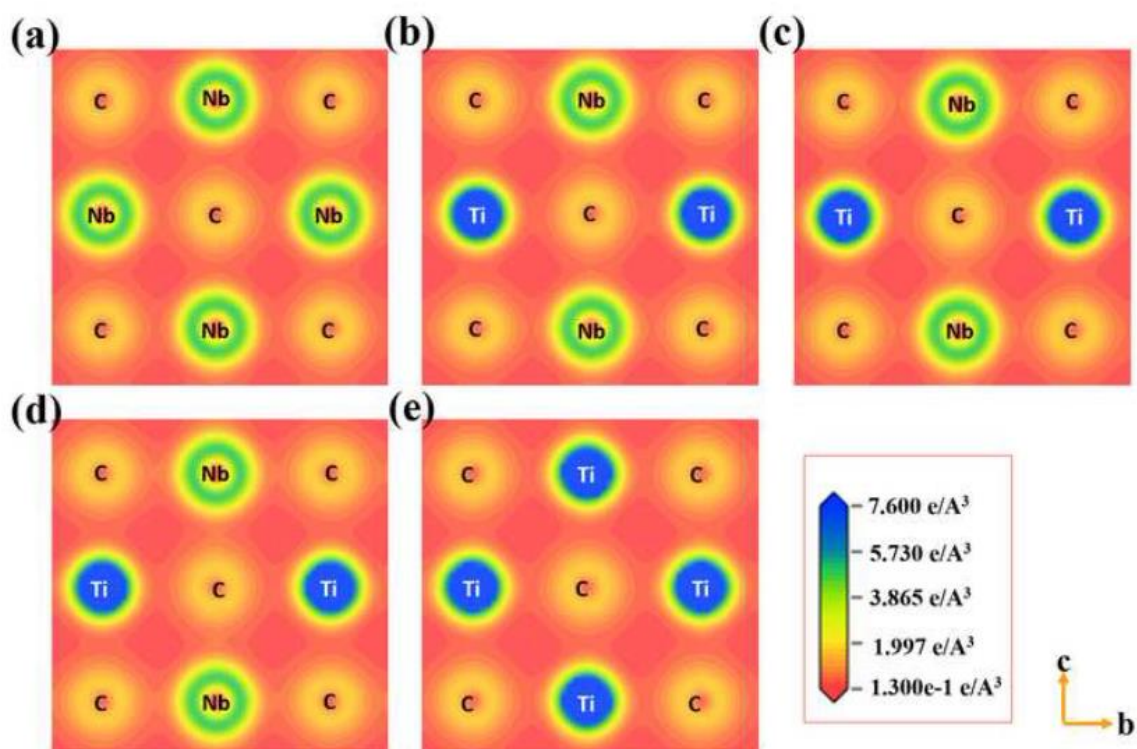
Fig.7. Theoretical hardness and brittleness of niobium carbides. (a) Theoretical hardness (b) Pugh's modulus ratio

Fig.8. Total and partial density of state (DOS) for (Nb,Ti)C. (a) NbC (b) $Nb_{0.75}Ti_{0.25}C$ (c) $Nb_{0.5}Ti_{0.5}C$ (d) $Nb_{0.25}Ti_{0.75}C$ (e) TiC

Fig.9. Charge density difference for (Nb,Ti)C taken along the (200) plane. (a) NbC (b) Nb$_{0.75}$Ti$_{0.25}$C (c) Nb$_{0.5}$Ti$_{0.5}$C (d) Nb$_{0.25}$Ti$_{0.75}$C (e) TiC

Fig.10. Charge density for (Nb,Ti)C taken along the (200) plane. (a) NbC (b) Nb$_{0.75}$Ti$_{0.25}$C (c) Nb$_{0.5}$Ti$_{0.5}$C (d) Nb$_{0.25}$Ti$_{0.75}$C (e) TiC